Quantitative magnetization measurements on nanometer ferromagnetic cobalt wires using electron holography

E. Snoeck
CEMES-CNRS, 29 rue J. Marvig, BP4347, 31055 Toulouse, France

R. E. Dunin-Borkowski[a)]
Department of Materials Science and Metallurgy, University of Cambridge, Pembroke Street, Cambridge CB2 3QZ, United Kingdom

F. Dumestre[b)] and P. Renaud
Digital DNA Labs, Semiconductor Products Sector, Motorola, le Mirail B.P. 1029, 31023 Toulouse Cedex, France

C. Amiens and B. Chaudret
LCC-CNRS, route de Narbone, 31055 Toulouse, France

P. Zurcher
Digital DNA Laboratories, Semiconductor Products Sector, Motorola, 2100 E. Elliot Road, Tempe, Arizona 85824

(Received 19 September 2002; accepted 1 November 2002)

The magnetic remanent states of 4-nm-diameter single-crystalline Co nanowires are characterized using off-axis electron holography. Measurements are obtained from isolated wires, as well as from bundles of wires and ''multibranch'' wires joined by 15-nm-diameter nodes of Co. The fraction of magnetically active moments in a single 4-nm-diameter wire is measured to be 1.01 ± 0.19, indicating that, to within experimental error, the wire is fully magnetized throughout its diameter.
 [DOI: 10.1063/1.1532754]

Nanometer diameter ferromagnetic wires are of interest because of their potential applications in magnetic recording and storage and because of the magnetic properties predicted for materials whose dimensions approach the atomic scale.[1–3] Techniques such as superconducting quantum interference device magnetometry have been used to measure the hysteresis loops of nanowires that are several tens of nm in diameter,[4] while the remanent magnetic states of wires that are several hundred nm in diameter have been characterized using magnetic force microscopy.[5]

Here, we use off-axis electron holography in the transmission electron microscope (TEM) to image the remanent states of 4-nm-diameter single-crystalline Co wires at room temperature. The technique allows the phase shift of a high-energy electron wave that has passed through a material to be recorded.[6] The phase shift ϕ is sensitive to electric[7,8] and magnetic[9,10] fields in the sample, and is given by the expression

$$\phi(x) = C_E \int V(x,z)dz - \frac{e}{\hbar} \int \int B_\perp(x,z)dxdz, \qquad (1)$$

where x is a direction in the plane of the sample, z is the incident electron beam direction, C_E is a constant that takes a value of 6.53×10^6 rad V^{-1} m^{-1} at a microscope accelerating voltage of 300 kV, V is the electrostatic potential, and $B_\perp$ is the component of the magnetic induction perpendicular to both x and z. For the nanowires of interest here, the electrostatic contribution to the phase shift is associated with the mean inner potential (MIP) (the composition and density) of the sample.[11]

Figure 1(a) shows schematic diagrams of the MIP and magnetic contributions to the phase shift for an infinitely long wire magnetized along its axis. The magnitudes of the two contributions to the phase, predicted using Eq. (1), are plotted for a Co wire in Fig. 1(b). $\Delta\phi_{\mathrm{MIP}}$ is plotted for an accelerating voltage of 300 kV for a MIP of Co of 26 V.[12] $\Delta\phi_{\mathrm{MAG}}$ is calculated on the assumption that $B = 1.7$ T. $\Delta\phi_{\mathrm{MIP}}$ and $\Delta\phi_{\mathrm{MAG}}$ vary linearly and quadratically with wire diameter, respectively, and are equal for a diameter of 84 nm. When the wire has a diameter of only 4 nm, $\Delta\phi_{\mathrm{MIP}}$ ($\pi/4.6$ radians) is predicted to dominate $\Delta\phi_{\mathrm{MAG}}$ ($\pi/98$ radians). For a wire of this diameter, the MIP contribution to the measured phase must, therefore, be removed if the magnetic signal is

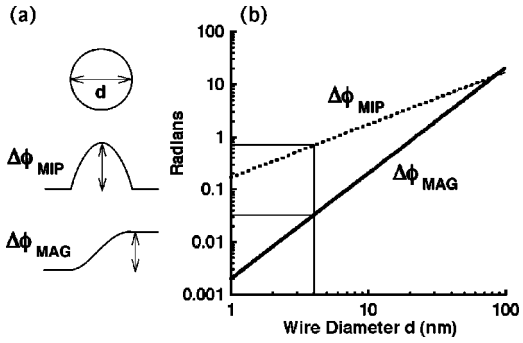

FIG. 1. (a) Schematic diagrams showing the MIP and magnetic (MAG) contributions to the phase shift of an electron wave that traverses a magnetic nanowire of diameter d. (b) Graph showing $\Delta\phi_{\mathrm{MIP}}$ (dotted line) and $\Delta\phi_{\mathrm{MAG}}$ (solid line) for a Co nanowire, plotted as a function of wire diameter.

a)Author to whom correspondence should be addressed; electronic mail: rafal.db@msm.cam.ac.uk
b)Also at: LCC-CNRS, route de Narbone, 31055 Toulouse, France.

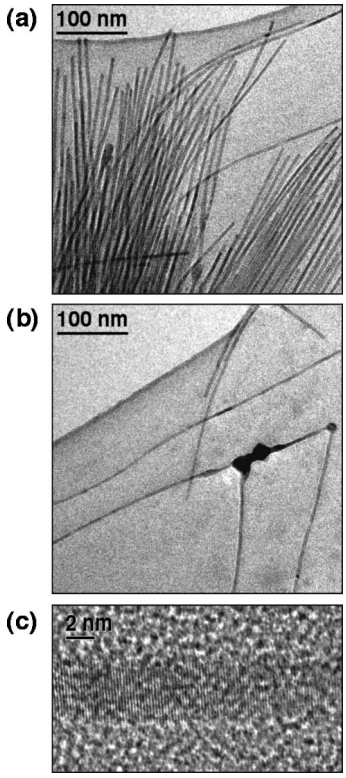

FIG. 2. Bright-field TEM images of (a) the end of a bundle of Co nanowires adjacent to a hole in the C support film, (b) a multibranch nanowire, comprising several nanowires joined together at junctions, and (c) [0002] Co lattice fringes visible along the length of an isolated wire.

to be quantified. Electron holography has previously only been used to characterize magnetic wires of significantly larger diameter.[13,14]

Figures 2(a)–2(c) show TEM bright-field images of the Co nanowires examined here. The wires were prepared by decomposition of the organometallic complex $Co(\eta^3-C_8H_{13})(\eta^4-C_8H_{12})$ in anisole at 150 °C under 3 bar of dihydrogen. The stabilizing medium comprised a mixture of oleic acid and oleylamine (2:1 acid:amine molar ratio).[15] The wires, which are 4 nm in diameter and up to several hundred μm in length, were kept under Ar until TEM examination to avoid oxidation. As well as isolated wires, bundles [Fig. 2(a)], and ''multibranch'' wires joined at ~15-nm-diameter nodes of Co [Fig. 2(b)] were characterized. Figure 2(c) confirms the presence of Co $c/2$ (0.204 nm) lattice fringes perpendicular to the axis of an isolated wire.

Electron holograms were recorded digitally at an accelerating voltage of 300 kV in a Philips CM300-ST field-emission gun TEM equipped with a Lorentz lens, an electrostatic biprism and a Gatan imaging filter 2000. Reference holograms from a vacuum were acquired to remove distortions associated with the imaging and recording system. Holograms were acquired with the sample in a low residual out-of-plane field of ~100 Oe, with the conventional microscope objective lens switched off. The magnetic contribution to the phase shift was obtained by recording two holograms of each area of interest, between which the Co wires were magnetized parallel and then antiparallel to their length by tilting the sample by $\pm 30°$ and switching the objective lens on fully to apply a large in-plane field of ~10 000 Oe to the sample.[16] The objective lens was then switched off and the sample returned to zero tilt to record each hologram. According to Eq. (1), half of the sum and half of the difference of the phase images obtained with the sample magnetized in opposite directions provide the MIP and magnetic contributions to the phase, respectively. This procedure requires alignment of the two phase images to subpixel accuracy, typically to better than ± 1 nm. Contours formed from the magnetic contribution to the phase provide a visual picture of the magnetic field in the sample. Their spacing is inversely proportional to the in-plane component of the induction integrated in the electron-beam direction.

Figure 3(a) shows a montage of holograms obtained from the end of a bundle of 4-nm-diameter Co nanowires. The boxes marked ''1'' and ''2'' correspond to the regions shown in Figs. 2(a) and 2(b), respectively. Figure 3(b) shows the magnetic contribution to the measured phase shift in the form of contours. The bundle of wires channels the magnetic flux along its length and, as it splits into two narrower bundles, the flux is channeled along these paths. Although the signal from the bundle appears to obscure that from individual wires and junctions, these details can be recovered by increasing the density of the contours. For example, Fig. 3(c) shows the box marked ''3'' in Fig. 3(b), but now with five times the density of contours. A junction of three wires can now be seen to be magnetized parallel to the applied field direction. The slight asymmetry between the contours on either side of the bundle in Fig. 3(b) may result from the effect of the leakage field of the bundle[17] on the reference wave. Figure 3(d) shows a line profile obtained from the magnetic contribution to the phase shift along the line marked ''4'' in Fig. 3(b). The step in phase across the bundle is (9.0 ± 0.2) radians. This value is consistent with the presence of (280 ± 7) ferromagnetically coupled wires, on the assumption that they each have a diameter of 4 nm and are uniformly magnetized with $B=1.7$ T.

Results from a single isolated wire and a multibranch wire are shown in Figs. 4(a) and 4(b) and 4(c) and 4(d), respectively. Figures 4(a) and 4(c) show the MIP contributions to the phase, while Figs. 4(b) and 4(d) show contours generated from the magnetic contributions to the phase [as in Fig. 3(b)]. The magnetic signal is weak and noisy, and was smoothed slightly before forming the contours. The contours visible along the length of the isolated wire confirm that it is magnetized along its axis. Although the magnetocrystalline easy axis coincides with the axis of each wire, the fact that this wire is magnetized along its length results primarily from its small diameter and high aspect ratio. The MIP and magnetic signals from the wire, which are shown in Figs. 4(e) and 4(f), respectively, have magnitudes of $\Delta\phi_{\mathrm{MIP}}=(0.65\pm 0.05)$ and $\Delta\phi_{\mathrm{MAG}}=(0.030\pm 0.005)$ radians, respectively. Rearrangement of Eq. (1) indicates that the fraction of magnetically active moments in the wire

$$f=\left(\frac{4\hbar C_E^2 V_0^2}{\pi e B}\right)\left(\frac{\Delta\phi_{\mathrm{MAG}}}{\Delta\phi_{\mathrm{MIP}}^2}\right) \tag{2}$$

takes a value of 1.01 ± 0.19 if $V_0=26$ V and $B=1.7$ T. This value for f is consistent with the presence of a material that has the magnetization of Co throughout the diameter of the wire (although an increased moment in a smaller diameter region cannot be ruled out).

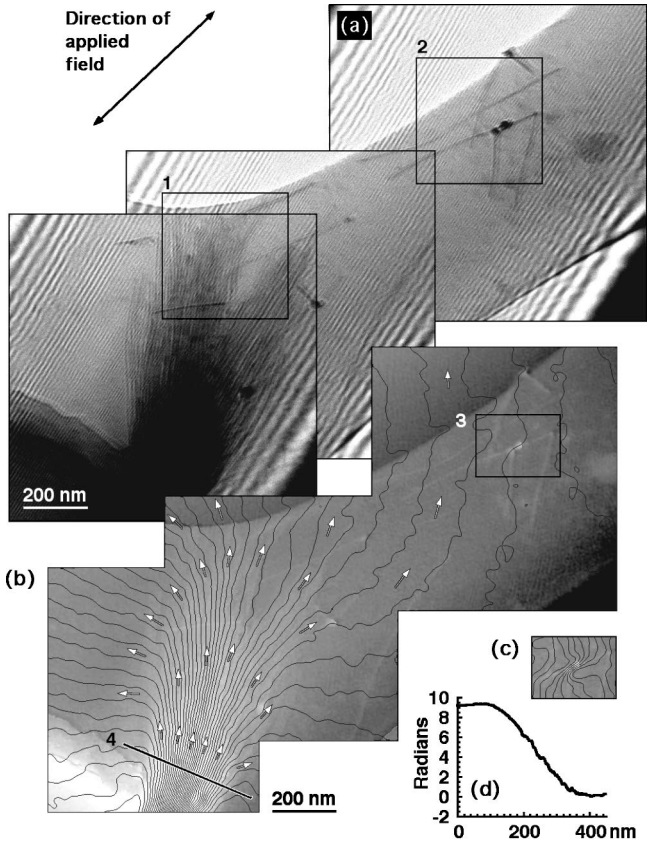

FIG. 3. (a) Montage of holograms of the end of a bundle of Co nanowires. The biprism voltage is 210 V, the acquisition time for each hologram 16 s, the holographic interference fringe spacing 3.9 nm, the field of view in each hologram 970 nm and the holographic overlap width 1160 nm. No objective aperture was used. (b) Magnetic remanent state, displayed in the form of contours (0.25 radian spacing) generated from the magnetic contribution to the holographic phase shift, after saturating the wires in the opposite directions marked at the top left-hand side. The contours are superimposed onto the MIP contribution to the phase shift. (c) As for (b), but for 0.05 radian contours obtained from region 3 in (b). (d) Line profile obtained from the magnetic contribution to the phase shift along the line marked 4 in (b).

In contrast, the magnetic signal from the multibranch wire shown in Fig. 4(d) is dominated by the junctions which are thicker in the electron-beam direction than the wires, and have a strong return flux around them. Line profiles obtained from the MIP and magnetic contributions to the phase, which are shown in Figs. 4(g) and 4(h), respectively, are consistent with junction diameters of approximately 15 nm. Further line profiles confirm that the wires that approach each junction are magnetized along their length. The magnetic signal is approximately an order of magnitude greater from the junctions than from the wires.

The fact that the contours are not straight in Fig. 4(b) is intriguing as magnetic ordering is expected to decrease as the dimensionality of a system is reduced.[18] The period of the distortion in Fig. 4(b) is approximately consistent with the activation volume predicted for magnetization reversal in Co wires of this diameter.[19] Similar effects have been reported for larger diameter polycrystalline Co (Ref. 20) wires. In the present case, the effect may arise from smoothing a weak signal or from diffraction contrast. In order to address these possibilities, noise may be decreased by examining wires suspended over a vacuum rather than over a C support film.

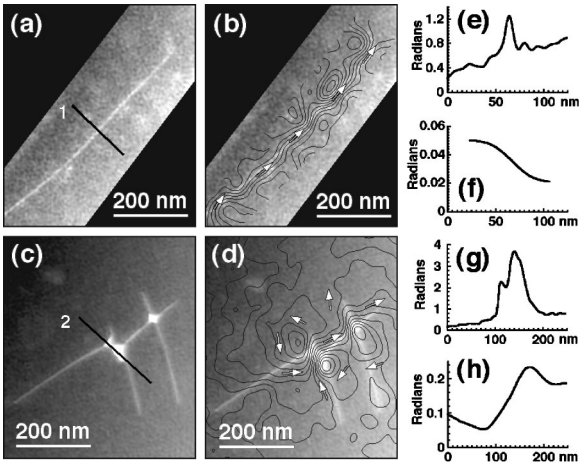

FIG. 4. (a) MIP contribution to the phase shift for a single Co nanowire. (b) Contours (0.005 radian spacing) generated from the magnetic contribution to the phase shift for the nanowire, superimposed onto the MIP contribution. (c) As for (a), but for a multibranch nanowire. (d) As for (b), but for the multibranch nanowire with a 0.015 radian contour spacing. (e, f) Line profiles obtained along line 1 from the MIP and magnetic contributions to the phase shift across the isolated nanowire, respectively. (f) was obtained by projecting (b) over a distance along the wire of ~200 nm. (g, h) As for (e, f), but for line 2 and the multibranch nanowire.

The authors are grateful to Professor M. R. Scheinfein and Dr. M. Respaud for discussions, and to the CNRS and the European Community for support through a European research network (GDR-E). One of the authors (R.E.D.) acknowledges the Royal Society for support.

[1] P. Gambardella, A. Dallmeyer, K. Maiti, M. C. Malagoli, W. Eberhardt, K. Kern, and C. Carbone, Nature (London) **416**, 301 (2002).
[2] F. J. Himpsel, J. E. Ortega, G. J. Mankey, and R. F. Willis, Adv. Phys. **47**, 511 (1998).
[3] M. Weinert and A. J. Freeman, J. Magn. Magn. Mater. **38**, 23 (1983).
[4] W. Wernsdorfer, K. Hasselbach, A. Benoit, B. Barbara, B. Doudin, J. Meier, J.-P. Ansermet, and D. Mailly, Phys. Rev. B **55**, 11552 (1997).
[5] K. Matsuyama, S. Komatsu, and Y. Nozaki, J. Appl. Phys. **87**, 4724 (2000).
[6] P. A. Midgley, Micron **32**, 167 (2001).
[7] W. D. Rau, P. Schwander, F. H. Baumann, W. Höppner, and A. Ourmazd, Phys. Rev. Lett. **82**, 2614 (1999).
[8] A. C. Twitchett, R. E. Dunin-Borkowski, and P. A. Midgley, Phys. Rev. Lett. **88**, 238302 (2002).
[9] A. Tonomura, Adv. Phys. **41**, 59 (1992).
[10] R. E. Dunin-Borkowski, M. R. McCartney, B. Kardynal, S. S. P. Parkin, and D. J. Smith, J. Microsc. **200**, 187 (2000).
[11] L. Reimer, *Transmission Electron Microscopy* (Springer, Berlin, 1997).
[12] M. de Graef, T. Nuhfer, and M. R. McCartney, J. Microsc. **194**, 84 (1999).
[13] C. Beeli, B. Doudin, J.-P. Ansermet, and P. A. Stadelmann, Ultramicroscopy **67**, 143 (1997).
[14] A. Sugawara, D. Streblechenko, M. R. McCartney, and M. R. Scheinfein, IEEE Trans. Magn. **34**, 1081 (1998).
[15] F. Dumestre, B. Chaudret, C. Amiens, M. C. Fromen, M. J. Casanove, P. Renaud, and P. Zurcher, Angew. Chem. **114**, 4462 (2002).
[16] R. E. Dunin-Borkowski, M. R. McCartney, D. J. Smith, and S. S P. Parkin, Ultramicroscopy **74**, 61 (1998).
[17] G. Matteucci, M. Muccini, and U. Hartmann, Phys. Rev. B **50**, 6823 (1994).
[18] L. D. Landau and E. M. Lifshitz, *Statistical Physics* (Pergamon, London, 1959), Vol. 5, p. 482.
[19] R. Skomski, H. Zeng, M. Zheng, and D. J. Sellmyer, Phys. Rev. B **62**, 3900 (2000).
[20] J.-E. Wegrowe, D. Kelly, A. Franck, S. E. Gilbert, and J.-P. Ansermet, Phys. Rev. Lett. **82**, 3681 (1999).